International Journal of Mechanical Engineering and Applications
2023; 11(5): 100-112
http://www.sciencepublishinggroup.com/j/ijmea
doi: 10.11648/j.ijmea.20231105.11
ISSN: 2330-023X (Print); ISSN: 2330-0248 (Online)

Welding Studies and Characterisation of Additively Manufactured LPBF Maraging Steel

Ramesh Kumar Saride[1, *], Srinivas Vajjala[1], Brijesh Patel[2], Suraj Kumar[1], Rajesh Kumar[1], Laxminarayana Pappula[3], Jagan Reddy Ginuga[1]

[1]Defence Metallurgical Research Laboratory, Hyderabad, India

[2]Defence Research and Development Laboratory, Hyderabad, India

[3]Department of Mechanical Engineering, Osmania University College of Engineering, Osmania University, Hyderabad, India

Email address:

srameshkumar.dmrl@gov.in (Ramesh Kumar Saride), srinivasv.dmrl@gov.in (Srinivas Vajjala), brijeshpatel.drdl@gov.in (Brijesh Patel), surajkumar.dmrl@gov.in (Suraj Kumar), rajesh.dmrl@gmail.com (Rajesh Kumar), laxp@osmania.ac.in (Laxminarayana Pappula), ginugajagan_61@yahoo.co.in (Jagan Reddy Ginuga)

[*]Corresponding author

To cite this article:

Ramesh Kumar Saride, Srinivas Vajjala, Brijesh Patel, Suraj Kumar, Rajesh Kumar, Laxminarayana Pappula, Jagan Reddy Ginuga. Welding Studies and Characterisation of Additively Manufactured LPBF Maraging Steel. *International Journal of Mechanical Engineering and Applications*. Vol. 11, No. 5, 2023, pp. 100-112. doi: 10.11648/j.ijmea.20231105.11

Received: August 6, 2023; **Accepted**: August 24, 2023; **Published**: September 8, 2023

Abstract: Additive manufacturing (AM) comes under the category of advanced manufacturing techniques that enables the manufacture of complex shaped components with reduction in multi-part assemblies, production lead times and weight. Maraging steel is a strategic material for manufacturing of components such as rocket motor casings, bulkheads etc. in defence and aerospace sectors. Laser Powder Bed Fusion (LPBF) AM technique has been explored in fabrication of Maraging steel components for end-use applications. In many applications, additively manufactured maraging steel parts are required to be welded to conventional material and it is important to understand weldability of these materials and their characteristics to ensure good bonding between the parts. It is also necessary to assess how welding process may affect the microstructure and consequently the mechanical properties of the AM maraging steel. In the present study, welding of AM maraging steel AM300 with conventional MDN250 was explored. With the available optimized parameters, maraging steel plates (160x100x6mm^3) were additively manufactured at low porosity without any defects of soot and spatter. The effect of heat treatment conditions on the volume fraction of reverted austenite in AM300 was also studied to arrive at an appropriate condition before carrying out the welding of AM300 plates. XRD and EBSD analysis revealed the formation of very fine reverted austenite in the as-deposited (AD) and Direct-aged (DA) conditions at the cell boundaries. Specimens when subjected to solution-treated and aged (STA) condition had almost eliminated the formation of reverted austenite at room temperature. Thus, the AM processed plates were subjected to solution treatment before carrying out the TIG welding of AM300 to MDN250 plates using W2 filler. Weldments of AM300-W2-MDN250 showed the formation of Fusion zone (FZ) and dark band Heat affected Zones (HAZ) on both the sides of FZ. Weld specimens subjected to ageing times at 490°C for 3.5hrs and 6hrs have shown similar average hardness values in AM300, FZ and MDN250 as 700HV, 675HV and 650HV respectively. Tensile strength and %El of as-welded, aged (3.5hrs) and aged (6hrs) specimens were evaluated to be 925MPa, 2.7%; 1730MPa, 2.4%; 1850MPa, 1.4% respectively. The tensile strength of AM300-W2-MDN250 weldment aged to 3.5hrs is found to be higher than that of conventional MDN250 weldment, but with about 60% reduction in ductility. However, higher weld strength being the main criteria, the joining of AM300 to MDN250 can be considered as a viable option for relevant applications.

Keywords: Additive Manufacturing, Laser Powder Bed Fusion, Maraging Steel, TIG Welding, Microstructural Characterization, Porosity

1. Introduction

Additive manufacturing (AM) technology is gaining importance in production of complex engineering components, especially in defence and aerospace industry. AM which is also known as 3D printing, is a process of building solid parts of any shape, layer-by-layer virtually from a digital model. The technology has many advantages over the conventional manufacturing like to realize complex designs, weight reduction, multiple prototypes/designs, reduction in lead time, etc., [1]. Additive manufacturing also comes as a ready solution to manufacture the components as conceptualized, designed and modeled by the designer. It gives a whole different degree of freedom for component design and designers no longer requires to follow the traditional philosophy of "Design for Manufacture", instead, they can follow a new philosophy of "Manufacture for Design" and create parts by means of better design that are lighter & stronger with improved durability, performance and efficiency [2].

Maraging steels are classified as ultra-high-strength carbon-free steels which exhibits excellent combination of high tensile strength and good fracture toughness [3]. This rare combination found with maraging steel makes it well suitable for safety-critical aerospace & defence structures such as rocket motor cases, missile casings, warhead shells, bulkheads etc., which require high strength along with damage tolerance. The massive increase in strength of maraging steel is due to the precipitation hardening caused by nanometric sized intermetallic particles which precipitates during subsequent aging of martensite in temperature range of 400-600°C [4]. During the solidification process of liquid metal into solid ingot, soft BCC martensitic structure of iron-nickel with supersaturated Co & Mo solid solution is obtained at RT. The subsequent aging treatment at an appropriate temperature and time duration hardens the matrix due to formation of Ni-Ti, Ni-Mo & Fe-Mo based nano-sized intermetallic precipitates in the martensitic structure.

Welding is a process of joining materials, usually metals, by application of heat with or without application of pressure and addition of filler material [5]. It is an essential process in manufacturing of components for creating strong and durable joints between materials. Proper welding techniques, along with careful selection of materials and process are important to ensure the strength, integrity and reliability of the final product. Good weldability with superior strength, fracture toughness and low specific weight of Maraging steel 300 makes it a suitable candidate for producing complex aerospace components using additive manufacturing technology. In many applications, additively manufactured maraging steel parts are required to be welded to conventional material and it is important to understand weldability of these materials, their characteristics to ensure good bonding between the parts. It is also necessary to assess how welding process may affect the microstructure and consequently the mechanical properties of AM materials. Welding and joining of additively manufactured maraging steel AM300 is therefore, an important area of research for various applications in the strategic sectors. Amongst the various existing joining techniques, TIG welding of maraging steel is widely used joining process due to its precise control, low heat input, low spatter and high quality of welded joints. Optimization of processing parameters of LPBF additively manufactured maraging steel and extensive characterisation is most vital to obtain good weldability and hence in achieving the final properties.

Sakai PR et al [6] highlighted that in Maraging steels it is essential to perform the aging after welding process. The reduction in yield and tensile strength were lower than 5% due to the welding process with loss of about 20% in ductility is attributed with formation of austenite in fused zone during the welding process. Kun Li et al [7] investigated the strength and toughness behavior of maraging steel welded by laser beam under different heat treatment conditions viz., aging (A), solutionizing + aging (SA) and homogenizing + solutionizing + aging (HSA). Microstructures of the weld metals with A and SA processes both comprised of finely dispersive Ni_3(Ti, Mo) precipitates, small martensite lath and reverted austenite along the grain boundary. However, in the weld metal with HSA process, it exhibited the same Ni_3(Ti, Mo) precipitate with the large martensite lath and the absence of reverted austenite. Renu N Gupta et al [8] highlighted Gas tungsten arc welding is commonly employed to fabricate thin walled maraging steel casings. However, sometimes, radiographic examination of welds revealed typical unacceptable indications requiring weld repair. It has been found that weld has a tendency to form typical Ca and Al oxide inclusions leading to the observed defects. Deepak P. et al [9] investigated Pulsed TIG bead-on-plate welding performed on a 5mm thick maraging C300 plate and arrived at optimum parameters. Deepak Kumar Gope et al. [10] analysed 5mm thick Maraging steel plates which were welded using GTAW process with maraging steel filler wire. PWHT at 480°C for 3hours shows significant improvement in its microstructure at FZ and HAZ and the grains become unidirectional. Hardness at FZ & HAZ decreased as compared to base metal mainly due to coarsening of grain structure. After PWHT, the hardness is significantly higher due to precipitate formation and finer grain structure. Tensile strength of PWHT sample found to higher due to precipitate formation.

Kun Li et al [11] highlighted that as the aging temperature increased, tensile strength of welded joints increased, reaching a maximum of 1640MPa at 520 °C, and then decreased. The static toughness of welded joints decreased at first and increased later with increase in aging temperature. Two types of reverted austenite found respectively in grain boundaries and in matrix of martensite, due to the change of aging temperatures. The Ni_3(Ti, Mo) precipitate and reverted austenite are the critical factors influencing the strength and toughness of welded joints. The Ni_3(Ti, Mo) precipitate in the weld metal improves the strength of welded joints remarkably as its volume fraction increases. The reverted austenite in

grain boundaries is harmful to the toughness, while the reverted austenite in the matrix is beneficial to the toughness because of its finely dispersive distribution and its positive effect on the release of the stress. Rajkumar V et al [12] investigated on Maraging steel weldments done by GTA welding technique. Block martensite was formed in the HAZ of the parent metal. Tension tests concluded that strain rate has considerable influence on the nature of ductility whereas it has very less influence on the tensile strength of Maraging steel. Correlation of microstructures with tensile property results has shown good agreement and gives better understanding. Shamantha et al [13] has investigated the welding of conventional MDN250 with W2 filler material in ST condition and aging the weldments to 480°C for 3hrs. The reported tensile properties of MDN250 weldment were YS-1440 MPa, UTS-1540 MPa, %El-6.5%.

From the literature survey, it is understood that the studies were mainly restricted to additive manufacturing of maraging steel, optimization of process parameters and mechanical property evaluation. As such there is sparse published work on the weldability of additively manufactured Maraging steel. Therefore, the present study was aimed to assess the weldability of additively manufactured maraging steel AM300 with conventional MDN250. In order to further process the AM300 material for welding studies, evaluation of reverted austenite in the AM processed maraging steel is also an important factor for study. Hence, the effect of heat treatment process on the volume fraction of reverted austenite in AM300 maraging steel was also considered as part of the current study. Furthermore, microstructural and mechanical property evaluation of welded joints of AM300 to conventional MDN250 has also been studied in detail.

2. Materials and Methods

2.1. Additive Manufacturing of AM300 Plate

Additive manufacturing of Maraging Steel AM300 plates were carried out using the STLR-400 metal LPBF facility from M/s Amace Solutions Pvt. Ltd., Bengaluru. Maraging steel powder AM300 in spherical form produced by Inert gas atomization process from Indo-MIM, Bengaluru was used for additive manufacturing of plates and specimens. Rolled plates of conventionally processed Maraging steel (MDN250) were obtained from Midhani, Hyderabad in solution annealed condition.

Initially, plates of dimensions 160x110x6mm^3 were additively manufactured using the optimized parameters obtained from DoE analysis as Laser power-210W, scan speed-835mm/sec, hatch width-30µm, scanning pattern-zig-zig at an energy density of 105J/mm^3. The scanning pattern was selected to move from left to right, i e., against the direction of gas flow and next layer was rotated 67° to the previous layer to minimize the residual stresses. The plates and specimens were printed in an atmosphere of Nitrogen gas flow. The preliminary trials of additive manufacturing of 2.5mm thin plates had resulted in high distortion due to the effect of thermal stresses formed during the process. Therefore, 6mm thick plates were built in AM, where no distortion was observed in the plate in as-deposited condition. This 6mm thick plate was then sectioned along thickness into two halves of about 2.5mm thickness for carrying out the welding studies.

2.2. Chemistry and Metallographic Examination

Chemical analysis of powders, AM300 plates and rolled plate was carried out on Inductively Coupled Plasma Optical Emission Spectroscopy (ICP-OES), Ultima Expert (HORIBA, France SAS make).

Specimens of size 20x20x2.5mm^3 were sectioned from the plate using wire cut EDM machine. The specimens were hot-mounted and ground with SiC papers from 220 to 1200 grit sizes. Subsequently, the diamond paste was used in a sequential manner with particle sizes of 9, 3 & 1µm to attain mirror-polished surfaces. Using the Leica-DM-6000M Optical micrography (OM) of these mirror-finished specimens was carried out to obtain images for porosity evaluation. Porosity analysis was carried out to determine the overall pore content using Image analysis technique. Finally, polished specimens were etched with the 3%Nital (97ml ethanol & 3ml nitric acid) solution to reveal the internal microstructure.

Further, microstructural examinations were carried out using Optical Microscopy and Scanning Electron Microscope (SEM- ZEISS SUPRA 55) on different specimens to observe the melt pool boundaries, sub-grain structure, micropores, inclusion, spatters and other defects.

2.3. Heat Treatment Studies

The as-deposited (AD) specimens were also subjected to various heat treatments, viz. Direct Aging (DA) at 490°C for 6hrs, Solution Treatment (ST) at 840°C for 1hr, Solution Treatment + Ageing at 490°C for 6hrs (STA) conditions. The purpose of carrying out the above treatments was to evaluate the volume fraction of Austenite (reverted) at different conditions. Reverted Austenite is a strength reducing phases in Maraging steel; hence it is desirable to keep it to the minimum levels.

2.4. Phase Analysis Using XRD and EBSD

AD, DA, ST and STA specimens were polished, light-etched in Nital solution to reveal the phase peaks when observed in XRD. To determine the phases present in specimen, a SmartLab X-Ray Diffractometer by Rigaku, Japan, with Co Kα (λ = 1.79A°) was used. The reason for using Co Kα was due to the presence of noise with Cu Kα (λ = 1.54Å), which makes it challenging to find the small peaks of austenite. The diffractometer operated at 40kV and 135mA, and data were collected in the range between 10° and 110° at a scan rate of 2°/min. The amount of phase present in all specimens was determined by one of the phase quantification methods, the Direct Comparison Method (Rietveld analysis), to compare the change in austenite content with heat treatment procedures.

Electron Back Scattered Diffraction (EBSD) was also performed on AD, DA, ST and STA specimens to identify the phase-fraction of austenite and martensite in a localized region. To obtain the smooth, scratch-free surface, specimens were cloth-polished up to 1µm using diamond paste and kept on VibroMet 2 Vibratory Polisher (manufactured by Buehler) for 8 hours. The analysis aimed to identify and quantify (by measuring the area fraction) the crystal structure, intermetallic precipitates, size, orientation, and morphology of grains and their position in the specimen. Before analysis, information such as configuration, space group, cell parameters, and others about phases was taken from Pearson Crystallographic Database and fed into the crystal structure database of the instrument. These phases include Iron (BCC), Iron (FCC), Ni_3Ti, Ni_3Mo, and Fe_7Mo_6.

2.5. Joining of Additive AM300 with Conventional MDN250

Initially plates of size (160x110x2.5mm^3) were cut from the conventionally processed MDN250. Traditionally, MDN250 plates were joined by TIG welding using a filler wire W2 for various applications. In a similar method, experimental trials were also conducted to perform manual TIG welding on AM300 plate with conventional MDN250. The bead-on-trials were performed initially on AM300 plate to assess the weldability with standard parameters used for TIG welding of conventional MDN250.

After successful bead-on-trials, TIG welding was carried out between two AM300 plates and later between AM300 and conventional MDN250 plates and carryout the welding studies. The edges of plates were machined to form a V-groove and W2 filler wire was passed along with the welding torch. A copper plate was placed at the bottom to act as heat sink to increase the solidification rate of weld pool and minimize the heat affected zone (HAZ).

The weld zone was slightly machined to mirror finish after the completion of welding, and then subjected to dye penetrant test and radiography to check for cracks and defects.

Specimens of size 35x10x2.5mm^3 were extracted using wire cut EDM for metallography analysis and microhardness testing.

2.6. Micro-Hardness Evaluation

Micro-hardness measurements were conducted in AD, ST and STA conditions on etched specimens using instrumented micro-indentation tester. Micro-indentations were performed edge to edge in the central region across the length of the specimen at an interval of 0.5/1mm. A Vickers diamond pyramid indenter was used to apply a 10N load with loading and unloading rates of 20N/min and a pause of 10secs after loading. At least 3 indentations were taken in a single position and average of the readings are plotted to obtain a hardness profile across the specimen length.

2.7. Evaluation of Tensile Properties

Flat tensile specimens were cut from the welded plates as per ASTM-E8 standard with a gauge length of 175mm and width 20mm. Instron testing equipment was used to perform the tensile tests on specimens in as-welded and aged conditions. The test data was evaluated to obtain the mechanical properties such as yield strength (YS), ultimate tensile strength (UTS), and % elongation (%El).

3. Results and Discussions

3.1. Chemical Analysis

The chemical composition of the Maraging steel AM300 powder, laser deposited specimens and W2 filler in weight percentage is shown in Table 1.

Table 1. *Chemical composition of AM300 powder and LPBF specimens.*

Element	ASTM A538 M300	AM300 Powder	LPBF specimen	W2 Filler wire
C	≤0.03	0.02	0.02	0.015
Si	≤0.10	0.17	0.14	--
Mn	≤0.10	0.04	0.02	0.01
P	≤0.01	0.0022	0.005	--
Cr	≤0.50	0.27	0.25	--
Mo	4.60-5.20	5.16	5.10	2.6
Ni	18.0-19.0	18.6	18.4	18.5
Ti	0.50-0.80	0.78	0.68	0.17
Al	0.05-0.15	0.054	0.05	0.5
Co	8.50-9.50	9.50	9.1	12.0
Fe	Bal	Bal	Bal	Bal

3.2. Additive Manufacturing of Plates

Figure 1 shows the additively manufactured plate (160x110x6mm^3) using laser powder bed fusion process. Initially, the plate was sectioned from the build plate at the base. Further, the additively manufactured plate (6mm thick) was cut into two halves along thickness, each about 2.5mm thick.

Figure 1. *Additively manufactured plate of size 160x100x6 mm^3.*

The plates were then solution treated (ST) in a vacuum furnace at 840°C for 1 hour so as to weld them with the rolled plate in a similar annealed condition. The initial trial of solution treatment of 2.5mm thick plates has resulted in some amount of distortion, which has been avoided in subsequent trials by placing non-reactive ceramic tiles as weights on the plates [Figure 2]. This has successfully resulted in obtaining solution-treated flat plates suitable to be taken up for TIG welding trials.

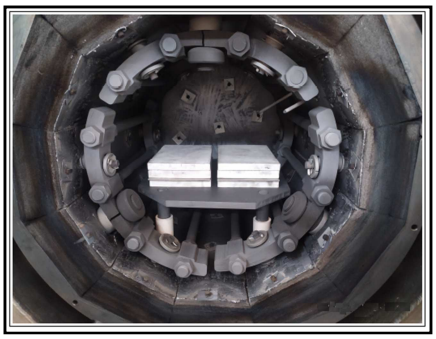

Figure 2. *ST of AM300 plate in vacuum furnace with weights placed.*

Figure 3a & 3b show the microstructure of specimen extracted from the ST plate (AM300-P) in polished and etched condition respectively. The presence of micro-pores could be observed from the images taken in polished condition. The microscopy image also confirms the absence of soot and spatter in the deposited material. From the image analysis method, the porosity in the specimen was determined to be ~0.16% in as-deposited condition, which is comparable to the porosity present in the as-cast condition. Hence, this solution treated AM300 plate can be considered for further welding trials using TIG welding process.

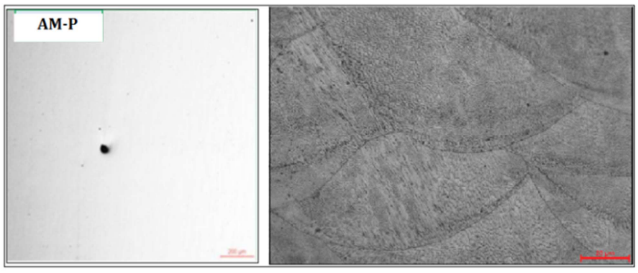

Figure 3. *(a) Optical image of polished specimen, (b) Etched at 500X.*

Along with the plates cube specimen (10x10x10mm^3) was also additively manufactured AM300-C as per the parameters shown in Table 2. Micro-hardness was carried out on cube specimen in AD and plate specimens both in AD and ST conditions.

Table 2. *Comparison of Porosity and Hardness for cube & plate specimens.*

Sample ID	Power (W)	Scan speed (mm/s)	Layer Thk (µm)	Hatch width (mm)	Porosity (%)	HVIT (HV10)
AM300-C-AD	210	835	30	0.08	0.12	368
AM300-P-AD	210	835	30	0.08	0.16	470
AM300-P-ST	210	835	30	0.08	0.16	360

It is observed that, in AD condition, the hardness in AM300 cube specimen is 368HV, whereas in AM300 plate specimen, it is found to be 470 HV. The difference of about 100 HV can be attributed to the formation of higher residual stresses due to the thin sectional thickness of the plate and the laser deposition processing on a large area. However, when hardness profile was obtained on the AM300 plate specimen in the ST condition, it is found to be 360HV, which confirms relieving of the residual stresses in this ST condition.

3.3. Microstructure of Conventional MDN250

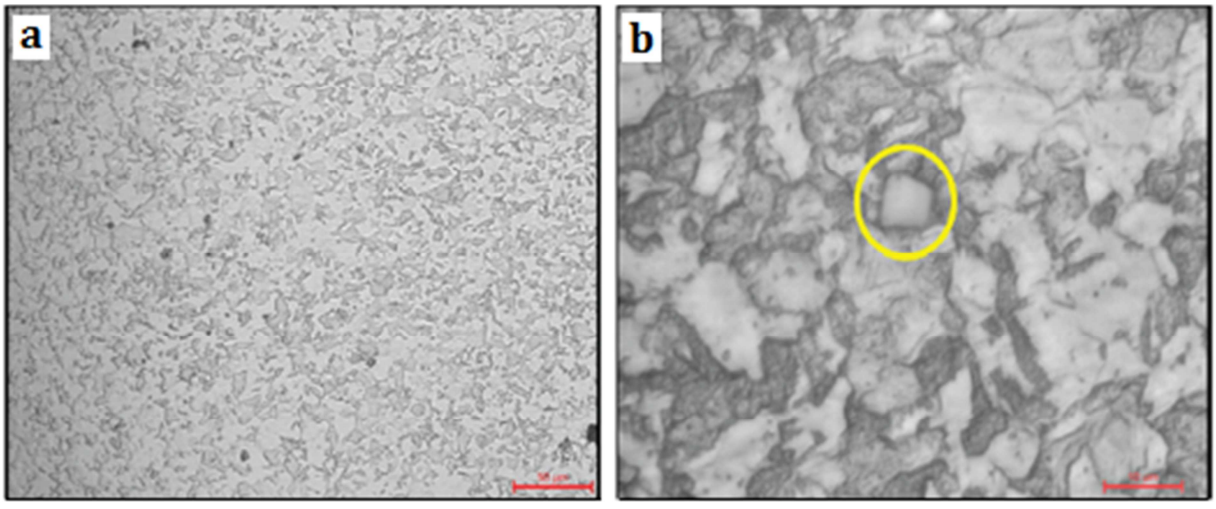

Figure 4. *OM of MDN250 200X and 1000X magnification.*

The optical micrograph of conventionally processed (rolled and annealed) MDN250 material used in the present study for welding trials is shown in Figure 4. From Figure 4a, it is observed that conventional MDN250 is comprised of equiaxed grain structure of BCC soft martensite. Figure 4b shows the presence of polyhedral particles (size ~5-8µm) embedded in the martensite matrix. Using SEM-EDX, elemental composition was extracted and particles were identified as TiN particles as shown in Figure 5. These particles were observed to be randomly spaced out in the matrix.

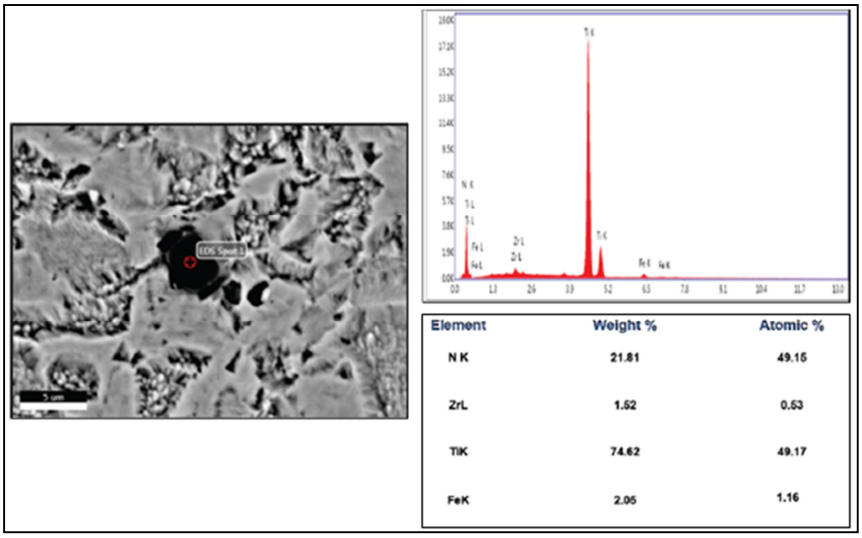

Figure 5. *EDX spot analysis on the polyhedral particle.*

3.4. XRD Analysis

Austenite reversion plays a vital role in determining its mechanical properties in maraging steel. With the increase in austenite content, the toughness of these steels increases but their mechanical strength decreases [14]. Austenite reversion occurs in every maraging steel, but extent of transformation depends on various factors such as time duration, the temperature of aging, cold work done on the material, and chemical composition of the steel. Rohit and Muktinutalapati [15] also observed an increase in the amount of reverted austenite with an increase in time and temperature of aging. At the beginning of aging, austenite pockets appear mainly at the boundaries of lath martensite and prior austenite grain boundaries. After that, these austenite pockets grow along the grain boundaries and nucleate within the martensite lath. For loss of strength, the contribution of reversion of martensite to austenite is more than the coarsening of precipitates [16].

The XRD peaks related to additively manufactured AM300 and conventional MDN250 (annealed) in AD, DA and STA conditions are plotted in Figure 6. Austenite peaks are designated as γ and Martensite peaks as α'. Austenite peaks are evidently present in the AM-P-AD and AM-P-DA specimens, whereas no such peaks could be detected in AM-P-STA and MDN250 specimens. It can be thus inferred that additively manufactured Maraging steel unavoidably contains some reverted austenite (4% by volume) due to the thermal cycling of layers which is intrinsic to the AM process. Further, Direct aging (DA) of AM specimens would only lead to the growth of Austenite phase particles resulting in increase of volume fraction to 7%. However, the absence of Austenite peaks in AM-STA and MDN250 (annealed) shows that solution treatment at above ~800°C and cooling in air to RT would convert most of the reverted Austenite to Martensitic structure. Table 3 gives the austenite volume percentage calculated using Reitveld analysis from the XRD peaks.

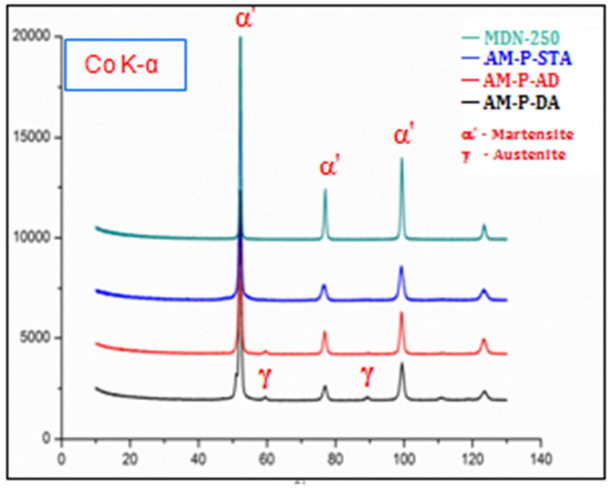

Figure 6. *XRD analysis of AM300 and conv. Maraging steel.*

Table 3. *Austenite (%) in AM-P and MDN250.*

S. No	Sample	Austenite (%)
1	AM-P-AD	4.4
2	AM-P-DA	7.0
3	AM-P-STA	<1
4	MDN250	<1

3.5. EBSD Phase Analysis

EBSD analysis shown in Figure 7 presents the microstructure taken from the plane parallel to the build direction of LPBF specimens. The as-deposited (AD) specimen was analyzed at a magnification of 1000X with a step size of 0.294µm. The colour phase map (Figure 7a) indicates the presence of very fine austenite (green) phase with the dominance of martensitic (red) phase. It can be observed in the band contrast map (Figure 7b), the finely distributed retained austenite (red) to have formed at cell boundaries. As mentioned earlier, thermal cycling or Intrinsic heat treatment (IHT) is the possible reason for the presence

of a small fraction of retained austenite in the AM processed specimens. IHT is reheating of the previously deposited layer when a new layer is being deposited in the LPBF process. Ahmadkhaniha et al. [17] also reported a similar observation and ascribed the reason to constant heat flow from molten regions to already deposited layer during the LPBF process. The Inverse Pole Figure (IPF) from Figure 7c depicts the randomized crystallographic orientation in AM processed maraging steel.

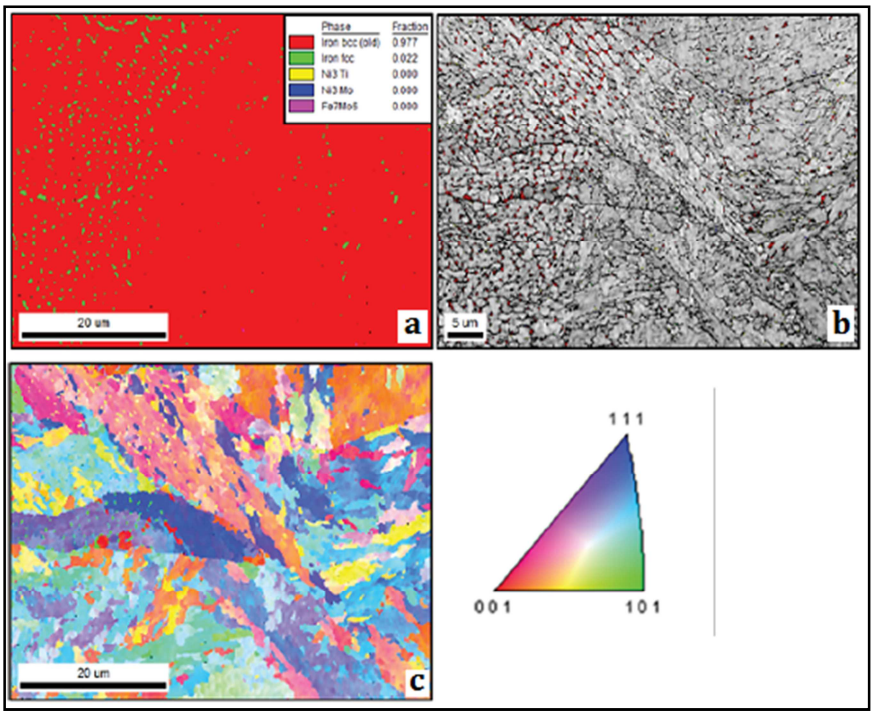

Figure 7. *(a) Phase colour map, (b) band contrast and (c) IPF.*

Figure 8 show a comparison of EBSD phase maps obtained from AD and DA specimens. It can be observed that the Austenite phase particles present at the cell boundaries in the AD specimen have grown in size during the direct ageing treatment. In contrast, Figure 9 shows that the reverted austenite formed during the AM process is almost eliminated by subsequent solution treatment + ageing condition. Also, the crystallographic orientation was observed to be randomized in STA condition. Therefore, it is necessary to solution treat (ST) the AM plates before carrying out the welding of AM Maraging steel to avoid the reverted austenite, which is detrimental in attaining the final mechanical properties. Hence, the AM300-P plate was subjected to Solution treatment in vacuum furnace before carrying out further welding studies.

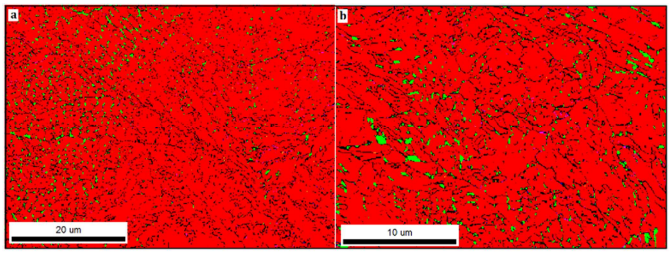

Figure 8. *EBSD phase map in (a) AD, (b) DA specimens.*

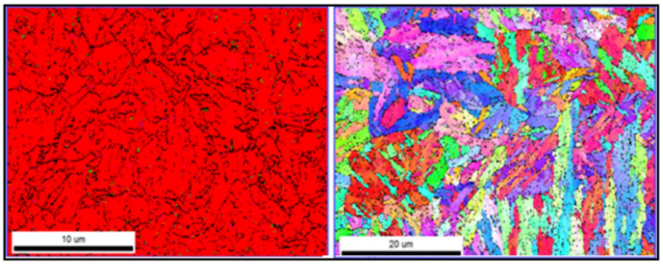

Figure 9. *EBSD phase map and IPF image in STA specimen).*

3.6. Welding Studies on AM300 Plate to MDN250 Plates

The Welding studies have been carried out on solution treated AM300 plates using manual TIG welding process. Two additively manufactured AM300-P1 and AM300-P2 plates were used to conduct the experimental trials. The welding studies have been carried out in stages as given below:

i. Run-on Bed Trials on AM300 Plate
ii. Welding of two AM300 plates
iii. Welding of AM300 with conventional MDN250 plates

3.7. Run-on Bead Trials on AM300 Plate

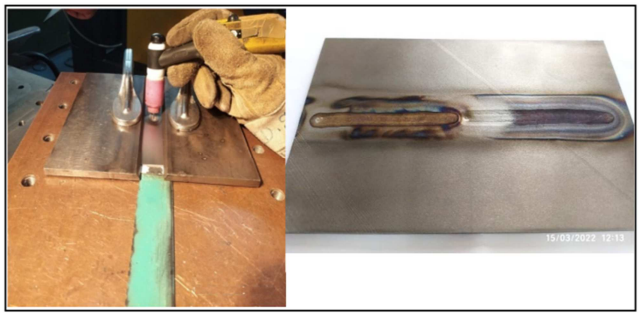

Figure 10. *Run-on-bead trial on AM300-P1 without filler.*

Initially, run-on-bead trials were carried out on AM300-P1 plate without filler using standard TIG welding parameters established for welding of conventional MDN250. Figure 10 above shows the actual run-on-bead experiment that has been carried out on AM300-P1.

Weld pass was carried out twice up to 70mm length in each pass. Subsequent characterization of weld beads through radiography and dye penetrant tests showed no detection of cracks and pores in both the passes.

3.8. Welding of Two AM300 Plates

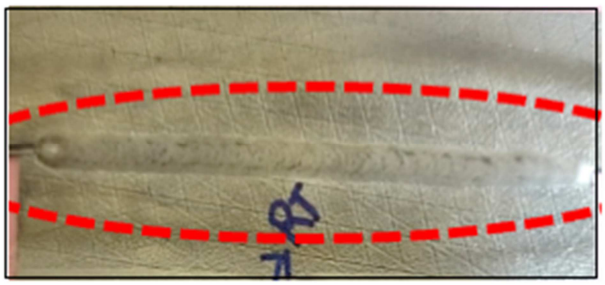

Figure 11. *Welding of AM300-P plates using W2 filler.*

In the next stage, welding of two additively manufactured AM300 plates of size 120x30x2.5mm^3 was carried out to study the weld feasibility using standard W2 filler with the same parameters (Figure 11). Standard edge preparation has been carried out at the edges of AM300 plates to form a V-groove for accommodating the filler wire. Subsequently, NDT tests through radiography and dye penetrant test showed no detection of cracks and pores across the weld-bead.

3.8.1. Microstructure Evaluation

Microstructural examination was carried out across the weld bead in plane parallel to plate thickness. The etched microstructure reveals formation of Fusion zone (FZ) in the weld bead followed by dark etched heat affected zones (HAZ) at 8mm distance from the center of fusion zone. Long columnar dendrites typical of cast structure are visible at the boundaries of the fusion zone (Figure 12a), whereas, fine cellular dendritic structure can be observed in the center of fusion zone (Figure 12b). At high magnification, the etched microstructure also reveals the presence of segregation at the cell boundaries in the fusion zone as seen by the white zones around the dark cell core (Figure 12c). The fusion zone comprises of a total width of 7mm.

Apart from the FZ in the weld bead, the plate is also affected by a HAZ on both the sides of FZ, which is revealed in etching by the presence of a dark band of 1mm width (Figure 12d). The heat from the weld bead was conducted to the bottom and sides of AM300 plate to the base copper plate, which results in attaining different temperatures at various positions across the width of AM300 plate. HAZ regions formed during the weld pass are those zones where the microstructure is affected by the transformation of phases, precipitation of intermetallics, etc., leading to a change in mechanical properties. The dark band HAZ (Figure 12d) indicates the change in microstructure which may affect the mechanical properties at the particular location.

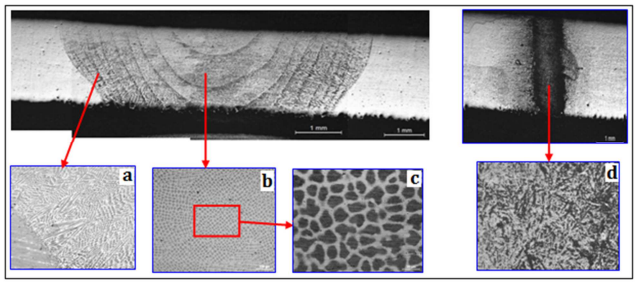

Figure 12. *Microsctructure of Weld bead and HAZ.*

3.8.2. Micro-Hardness Evaluation

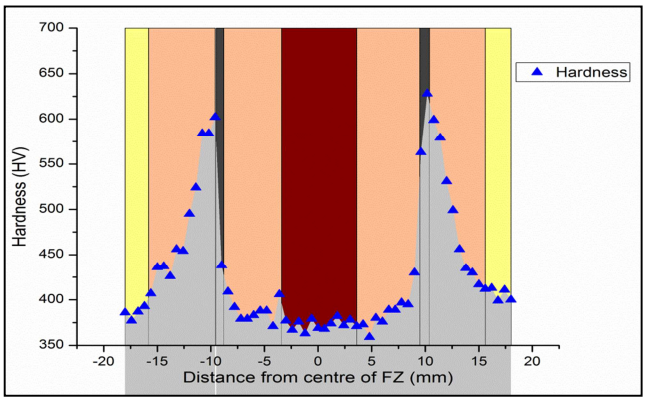

Figure 13. *Micro-hardness along welded region in as welded condition.*

Micro-hardness profile taken across the length of the cut

section using instrumented indentation tester is shown in Figure 13. The hardness profile shows that hardness in the fusion zone is ~360HV equivalent to that of annealed MDN250. A hardness of ~620 HV was observed in the dark band HAZ. From the HAZ, hardness variation was found to gradually decrease from 620 to 400HV in a span of ~5mm. This can be attributed to the phenomenon of age-hardening taking place at different levels in these zones depending on the temperature and time of exposure. Such hardness behavior is observed symmetrically on either side of the fusion zone.

3.9. Welding of AM300 Plate with Conventional MDN250

Majority of the applications demand welding of additively manufactured Maraging steel AM300 to the assembly comprising of conventionally manufactured MDN250 grade Maraging steel. Therefore, further study has been carried out on welding of AM300 plate to that of conventional MDN250 plates. Figure 14a shows the actual welding of 160x110x2.5 mm^3 AM300-P plate with conventional MDN250 plate with the same welding parameters with W2 filler wire. Figure 14b shows the weld bead and the heat affected region surrounding the weld bead across the length of the plates. The NDT tests through radiography and dye penetrant test showed no defects across the weld. Specimens were extracted laterally (marked in red) using EDM wire cut for metallography, hardness and tensile property evaluation. The tensile specimens were extracted in such a manner so as to ensure that the weld bead position is in the center of the gauge length. Since, the welding was carried out on the AM300-P and MDN250 plates in the ST condition, the specimens were later subjected to age-hardening treatment at 490°C for two time intervals, i e 3.5hrs and 6hrs also to understand the effect of ageing time duration on mechanical properties.

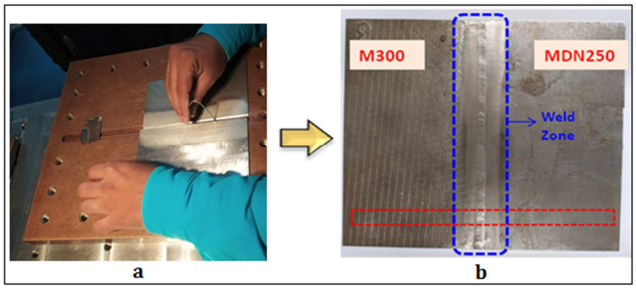

Figure 14. *Welding of AM300 Plate with conventional MDN250.*

3.9.1. Microstructure Evaluation

Specimens of size 35x10x2.5mm^3 were extracted using wire cut EDM for metallography analysis and microhardness testing. The optical microscopy images were taken throughout the length of the sectioned specimen and merged together for a panoramic view (Figure 15) of the welded specimen. Figures 15 a, b & c show the etched microstructures, HAZ-1 in the AM300, FZ in the weld bead and HAZ-2 in the MDN250 respectively. As observed in the welding of two AM300 plates, a similar microstructure was obtained in welding of AM300 plate with conventional MDN250. Dark HAZ-1 and HAZ-2 bands of about 1mm width were formed in both AM300 and MDN250 plates respectively at a distance of 8mm from the fusion zone center. In the as-welded condition, the FZ comprises of cellular dendrites at the center with elemental segregation at the cell boundaries, whereas the HAZ zones comprise of very fine cellular regions.

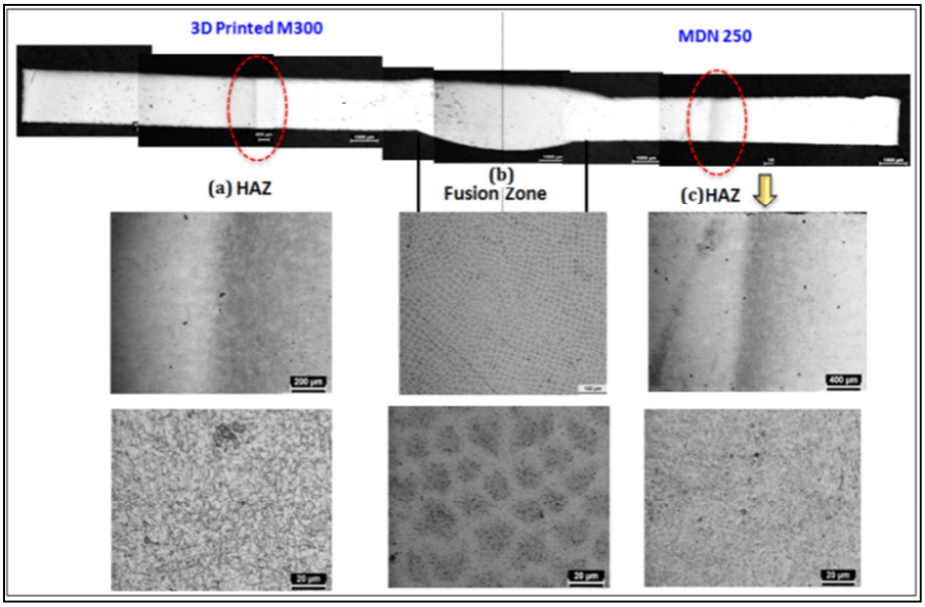

Figure 15. *Microstructure of weld section in as-welded condition, a) HAZ in AM300, b) Fusion zone, c) HAZ in MDN250.*

Figure 16 a & b show the image of fusion zone in the as-welded and aswelded+aged condition at 490°C, 6hrs. The aged specimen revealed the formation of bright precipitates of reverted austenite in the cell boundaries (marked in red). The

segregation of heavy elements (Ni etc.) at the cell boundaries would enhance the formation of reverted austenite during aging.

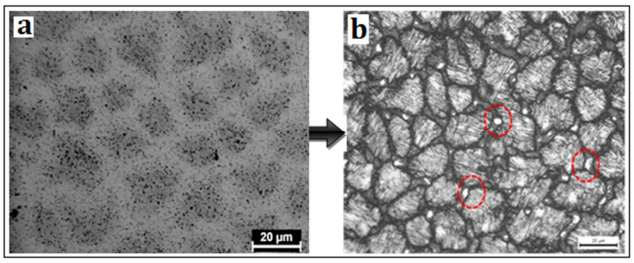

Figure 16. *Microstructure of (a) as-welded and (b) aged specimens in FZ.*

3.9.2. Mechanical Properties

Specimens Micro-hardness profile was taken across the length of cut section in the as-welded condition at an interval of 0.5mm. The hardness profile (Figure 17) shows that FZ region attained a hardness of 350HV, whereas the peak hardness attained in HAZ1 of AM300 and HAZ2 of MDN250 were 625HV and 500HV respectively. A gradual decline in hardness was observed in moving away at both the HAZ regions to ~400 HV. The difference in peak hardness values of HAZ-1 and HAZ-2 can be attributed to the actual variation in hardness of AM300 and MDN250 materials.

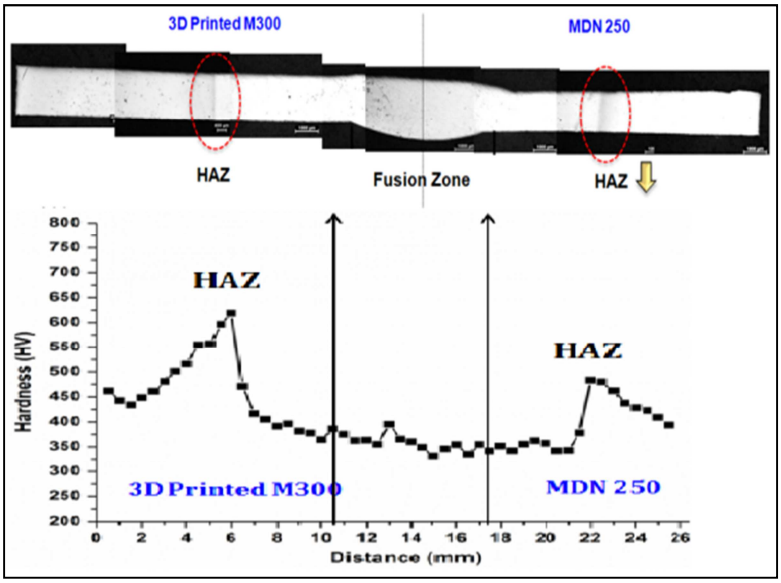

Figure 17. *Microhardness profile along the welded region of AM300 and MDN250 in as-welded condition.*

A comparison of hardness profile in as-welded and aged condition (3.5hrs) was depicted in Figure 18. Upon aging to 3.5hrs, the hardness of the entire specimen has increased to above 600HV due to formation of nano-precipitates. However, it can also be observed that the regions in the HAZ dark band showed signs of decreased hardness possibly due to over-aging phenomenon. The average hardness attained amongst AM300, Fusion Zone and MDN250 is about 700 HV, 675 HV and 650 HV respectively.

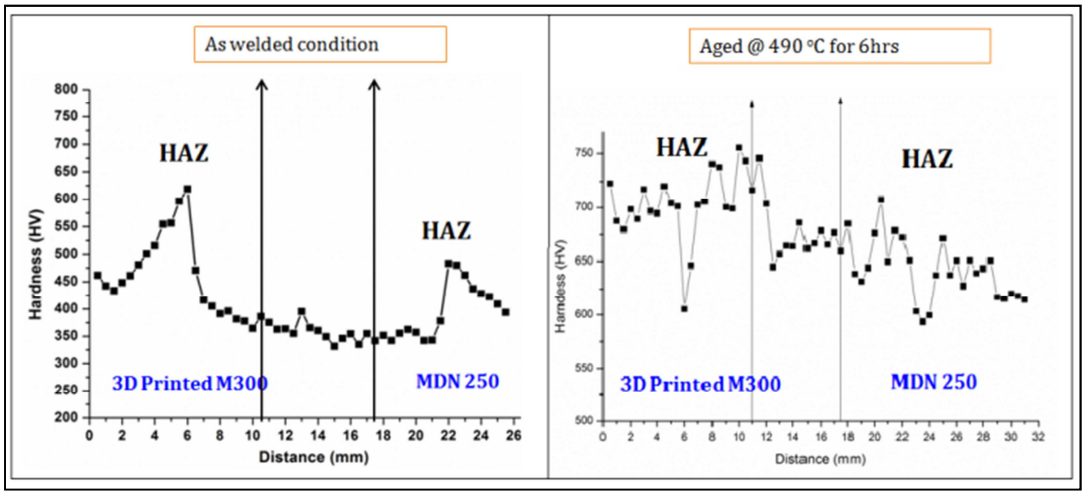

Figure 18. *Comparison of Microhardness profile in As welded and Aged @ 3.5hrs along the welded region of AM300 and MDN250.*

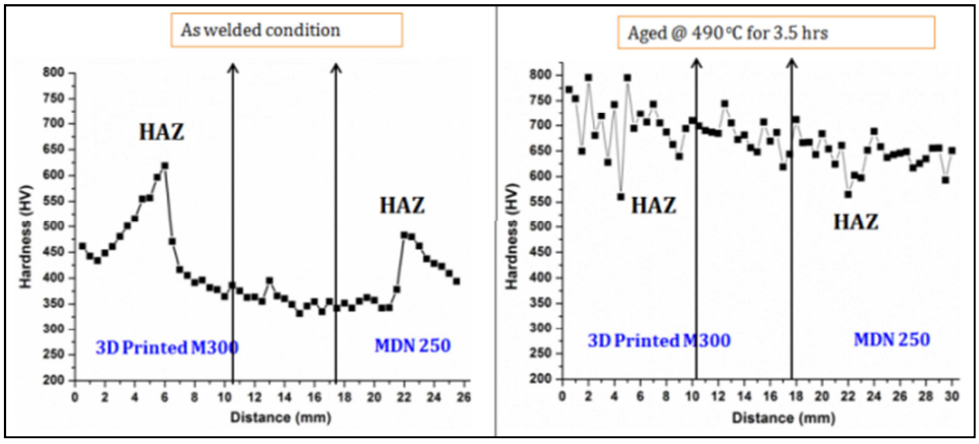

Figure 19. *Comparison of Microhardness profile in As welded and Aged @ 6hrs along the welded region of AM300 and MDN250.*

A similar comparison of hardness profile in as-welded and aged condition (6hrs.) was observed as shown in Figure 19. Even after ageing to 6hrs the average hardness attained amongst AM300, Fusion Zone and MDN250 is about 700HV, 675HV and 650HV respectively. Hence it can be inferred that there is no significant difference in hardness profiles of aswelded + aged specimens at 3.5hrs and 6hrs of ageing times.

Tensile properties were evaluated for as-welded, welded+aged (3.5hrs), welded+aged (6hrs) on the flat tensile specimens extracted across the weld joint. Figure 20 shows the actual flat tensile specimens tested and locations of failure. It can be observed that all the specimens in all 3 conditions have failed in the fusion zone only, but with different failure modes. Table 4 gives the average values of the tensile results carried out on specimens in the 3 conditions.

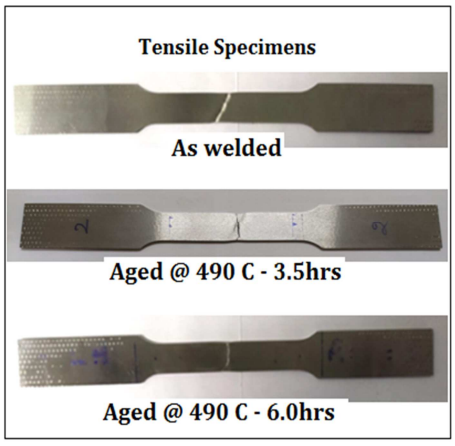

Figure 20. *Fractured specimens in different conditions.*

Table 4. *Tensile properties of specimens in different conditions.*

Property	As Welded Specimen	Aged @ 3.5hrs specimen	Aged @ 6.0hrs specimen
0.2% YS	870 MPa	1710	1810 MPa
UTS	925 MPa	1730	1850 MPa
%El	2.7 %	2.4 %	1.4%
Hardness (FZ)	350 HV	675 HV	675 HV
Failure	FZ	FZ	FZ
Mode of fracture	Ductile	Brittle	Brittle

The as-welded specimen showed an elongation of 2.7% with ductile fracture mode, whereas, as anticipated after ageing, the strength increases to 1730MPa with a reduction in ductility to 2.4% in aged (3.5hrs) specimen. The strength further increased to 1850MPa while the ductility reduced to 1.4% in aged (6hrs) specimen. Though no significant change in hardness was observed between aged (3.5hrs and 6hrs) specimens, considerable variation in strength and ductility was obtained. The poor ductility and brittle failure of aged (6hrs) specimen may be due to formation of coarse precipitates at the cell boundaries in fusion zone which are the potential regions of crack initiation. Hence, it can be inferred that as-welded plates can be subjected to 3.5hrs of ageing to achieve optimal tensile properties of strength and ductility.

From the welding studies it can be concluded that additively manufactured AM300 can be successfully welded with conventional MDN250 material in ST condition using standard W2 filler. The results obtained by Shamantha et al [13] in the conventional MDN250 weldments were YS-1440MPa, UTS-1540MPa, El-6.5%. In comparison to this, weldment of AM300 to MDN250 using W2 filler aged to 3.5hrs at 490°C has shown YS-1710MPa, UTS-1730MPa and El-2.5%. Though the yield and tensile strength have increased, there is degradation in ductility which may be due to the impurities or defects arising in the AM processed maraging steel. Besides, higher grade AM300 also possesses higher strength and lower ductility compared to MDN250. Further work involves high-end microstructural investigations to look into the causes for low ductility of additively manufactured maraging steel when compared to conventional material. The fracture toughness is also a vital property of Maraging steel for practical applications. Hence, evaluation of fracture toughness in additively manufactured Maraging steel needs to be investigated.

4. Conclusion

Following conclusions were drawn from the present study of welding of additively manufactured and conventional maraging steel:

1. Plates of size 160x100x6mm^3 and cube specimen (10x10x10mm^3) were additively manufactured at

reduced porosity (~0.1%) without any defects of soot and spatter. Micro-hardness was found to be 100HV higher in plates than cube specimens due to higher residual stresses generated as a consequence of depositing lower sectional thickness and also large area of deposition.

2. XRD and EBSD analysis revealed the formation of very fine reverted austenite in the AD and DA condition at the cell boundaries. Thermal cycling or intrinsic heat treatment, which is inherent to AM processing, is the possible cause for the presence of a small fraction of retained austenite.
3. Specimens when subjected to STA condition almost eliminated the formation of reverted austenite at RT. Therefore, it is necessary to carry out the welding of AM processed Maraging steel in ST condition to eliminate the presence of reverted austenite in the subsequent ageing process.
4. Weld bead trials on AM300-P plates showed formation of Fusion zone (FZ) and dark band Heat affected Zones (HAZ) on both the sides of FZ. The FZ region possessed hardness of 360HV with segregation of heavy elements at cell boundaries. A hardness of 620HV was observed in the dark band HAZ and found to be gradually decreased from 620 to 400HV in a span of ~5mm away from the weld. This can be attributed to the phenomenon of age-hardening taking place at different levels in these zones depending on the temperature and time of exposure.
5. Welding of AM300 plate to conventional MDN250 has been carried out and similar microstructural and hardness profiles were found, as observed in welding of AM300 plates in as-welded condition. Weld specimens subjected to ageing times for 3.5hrs and 6hrs showed average hardness values in AM300, Fusion Zone & MDN250 at about 700HV, 675HV & 650HV respectively with no significant difference in hardness profiles.
6. Tensile strength and %Elongation of as welded, aged (3.5hrs) and aged (6hrs) specimens were evaluated to be 925MPa, 2.7%; 1730MPa, 2.4%; 1850MPa, 1.4% respectively. Though no significant change in hardness was observed between two conditions of aged specimens, considerable variation in strength and ductility was observed. The poor ductility of aged (6hrs) specimen may be due to coarse precipitates at the cell boundaries in the fusion zone which are the potential regions of crack initiation. Hence, as-welded plates may be subjected to 3.5hrs of ageing to achieve optimal tensile properties of strength and ductility.
7. Additively manufactured AM300 can be successfully welded in ST condition with conventional MDN250 material using standard W2 filler. The tensile strength is found to be higher than that of conventional MDN250 weldments, but with about 60% reduction in ductility. However, higher weld strength being the main criteria, the joining of AM300 to MDN250 can be considered as a viable option for relevant applications.

Acknowledgements

Authors are extremely thankful to Director, DMRL for his unstinted encouragement in the Additive Manufacturing activities. Authors also thank M/s Amace Solutions Pvt. Ltd., Bengaluru for providing the additively manufactured specimens for the present study. Thanks are also due to other groups of DMRL viz., MBG, EMG & SFAG for extending necessary technical services.

References

[1] Mercedes Pérez, Diego Carou, Eva María Rubio & Roberto Teti. (2020). “Current advances in additive manufacturing”. 13th CIRP Conference on Intelligent Computation in Manufacturing Engineering, CIRP ICME '19, Procedia CIRP 88. 439–444.

[2] Brett P Conner, Guha P Manogharan, Ashley N Martof, Lauren M Rodomsky, Caitlyn M Rodomsky, Dakesha C, Jordan & James W Limperos. (2014). “Making sense of 3D printing: Creating a map of additive manufacturing products and services”, Additive Manufacturing, Vol 1-4, 64-76.

[3] W. M. Garrison, May K. Banerje. (2001). “Martensitic Non-stainless Steels: High Strength and High Alloy”. Encyclopedia of Materials: Science and Technology, P5197-5202, doi.org/10.1016/B978-0-12-803581-8.02519-4.

[4] Daniela Passarelo Moura da Fonsecaa Ana Larissa Melo Feitosaa Leandro Gomes de Carvalhob*, Ronald Lesley Plauta Angelo Fernando Padilha. (2021). “A Short Review on Ultra-High-Strength Maraging Steels and Future Perspectives. Materials Research”. 24 (1): e20200470, doi.org/10.1590/1980-5373-MR-2020-0470

[5] FC Campbell. (2011). “Joining – Understanding the basics”, ASM International, The Materials Information Society. ISBN 978-1-61503-825-1.

[6] Sakai PR, Lima, MSF, Fanton, L, Gomes CV, Lombardo S, Silva DF, Abdalla AJ. (2015). “Comparison of Mechanical and Microstructural Characteristics in Maraging 300 Steel Welded by three different processes: LASER, PLASMA and TIG”. Procedia Engineering 114 291–297.

[7] Kun Li, Jiguo Shan, Chunxu Wang, Zhiling Tian. (2016). “Effect of post-weld heat treatments on strength and toughness behavior of T-250 maraging steel welded by laser beam”. Materials Science & Engineering A 663, 157–165, www.elsevier.com/locate/msea

[8] Renu N Gupta, VS Raja, MK Mukherjee, and SVS Narayana Murty. (2017). “On Improving the Quality of Gas Tungsten Arc Welded 18Ni 250 Maraging Steel Rocket Motor Casings”. Metallurgical and Materials Transactions A, Volume 48A, 4655-4666.

[9] P Deepak, M J Jualeash, J Jishnu, P Srinivasan, M Arivarasu, R Padmanaban and S Thirumalini. (2016). “Optimization of process parameters of pulsed TIG welded maraging steel C300”. IOP Conf. Series: Materials Science and Engineering 149, 012007 doi: 10.1088/1757-899X/149/1/012007

[10] Deepak Kumar Gope, Priyanshu Kumar, Somnath Chattopadhyaya, Gowrishankar Wuriti, Tessy Thomas. (2021). "An investigation into microstructure and mechanical properties of maraging steel weldment". IOP Conference Series: Materials Science and Engineering 1104, 012014, doi: 10.1088/1757-899X/1104/1/012014.

[11] Kun Li, Jiguo Shan, Chunxu Wang, Zhiling Tian. (2016). "Influence of aging temperature on strength and toughness of laser-welded T-250 maraging steel joint". Materials Science & Engineering A 669, 58–65.

[12] Rajkumar. V, Arivazhagan. N, Devendranath Ramkumar. K. (2014). "Studies on welding of maraging steels". MRS Singapore-ICMAT Symposia Proceedings 7th International conf. on materials for advanced technology, Procedia Engineering 75, 83-87.

[13] C. R. Shamantha, R. Narayanan, K. J. L. Iyer, V. M. Radhakrishnan, S. K. Seshadri, S. Sundararajan & S. Sundaresan. (2000). "Tensile properties and fracture toughness of18Ni (250 grade) maraging steel weldments". Science and Technology of Welding and Joining, 5: 5, 329-337, doi: 10.1179/136217100101538399.

[14] Viswanathan, U. K., Dey, G. K., and Asundi, M. K. (1993). "Precipitation Hardening in 350 Grade Maraging Steel". Metallurgical and Materials Transactions A, 24 (11), 2429–2442.

[15] Rohit, B., and Muktinutalapati, N. R. (2018)."Austenite reversion in 18% Ni maraging steel and its weldments". Materials Science and Technology, 34 (3), 253–260.

[16] Schnitzer, R., Radis, R., Nöhrer, M., Schober, M., Hochfellner, R., Zinner, S., Povoden-Karadeniz, E., Kozeschnik, E., and Leitner, H. (2010). "Reverted austenite in PH 13-8 Mo maraging steels". Materials Chemistry and Physics, 122 (1), 138–145.

[17] D. Ahmadkhaniha, H. Moller, & C. Zanella. (2021). "Studying the Microstructural Effect of Selective Laser Melting and Electropolishing on the Performance of Maraging Steel". Journal of Materials Engineering and Performance. Volume 30 (9), 6588-6605.